2015 IEEE International Conference on Robotics and Automation (ICRA)
Washington State Convention Center
Seattle, Washington, May 26-30, 2015

Design and Control of a Novel Multi-state Compliant Safe Joint for Robotic Surgery

Zerui Wang, Peng Li, David Navarro-Alarcon, Hiu Man Yip, Yun-hui Liu, Weiyang Lin and Luyang Li

***Abstract*—In this paper, we propose a novel design of compliant safe joint, which has flexibility when the work load exceeds a predefined threshold. The compliance is generated by a spring. We design a special transmission mechanism to convert axial motion into circumferential motion such that the linear compliance can be converted into circular one. When the end-effector of a surgical robot actuated by the compliant safe joints collides with patient's body, the compliance of the joints will protect the patient by absorbing part of the collision energy. Because of the system's special mechanical structure, the control methods should be different when it works under different states. We propose a simple algorithm to choose control methods so that the system can work both under rigid and flexible states with different controllers. We have built a prototype to validate the design and the controller.**

I. Introduction

With the incorporation of robotics in our daily life, attention had been paid to the safety issues related to physical interaction between human beings and robots. [1]–[3]. Especially in surgical robots, where human-robot interactions are inevitable when surgeons use them to perform surgeries, the safety requirements are much stricter. Compliant joints can help to reduce the force acting on human body by absorbing part of energy during collisions or contacts.

To cope with these issues, there are mainly two kinds of methods to produce compliance in a system: (1) in active systems, compliant nature is produced from the algorithm of control system rather than from mechanical structure [4], [5] and (2) in passive systems, the compliant nature is produced from the mechanical structure rather than from the control system. The two kinds of compliance were compared in [6]. Active compliant system has high programming ability and some limitations like delayed contact response, low reliability, high cost and complex control algorithms. A passive compliant system often provides faster and more reliable response to dynamic collision than an active system. Because the compliant safe joint is designed for the robotic surgery, the reliability and response time are important. Therefore, we incorporate compliance into the system in a passive way.

Introducing compliance in actuator leads some control problems, which have been studied by many researchers. In [7], Spong provided two control methods of robot manipulators with elastic joints. They used feedback linearization and singular perturbation formulation. Tomei used a PD controller to robot manipulators with elastic joints from point to point, and also proved the stability of the system [8]. An inversion algorithm was introduced, by Luca *et al*. in [9], for the synthesis of a dynamic feedback control law to get full state linearization. Vallery *et al* have analyzed and compared several control strategies [10]. Meanwhile, many actuators with passive compliance have also been developed by many researchers, e.g., [11]–[17]. The robot joints mentioned above do have some compliance and some of them even have adjustable compliance. However, they have several drawbacks: (1) most of them have big volume, which leads the difficulty in applications; (2) they have only one working state, and the joints will always work with compliance.

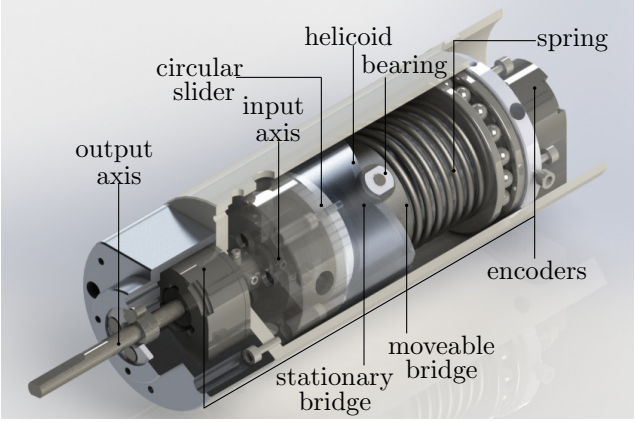

Fig. 1. A sectioned view of the CSJ's assembly.

In this paper, we present a novel design of compliant safe joint which has a compact structure leading to small volume. One of the novelties is that the joint can work as rigid joint when the work load is smaller than the threshold and will shift into flexible state, when the work load exceeds the threshold. By introducing the switching algorithm, our approach can control the joint both under rigid and flexible states. We report experiments with a compliant safe joint prototype to validate the design and also the control approach. We also report an ex vivo experiment, in which our surgical robot was actuated by compliant safe joints.

The rest of this manuscript has the following structure: In Section II, we explain the design details of compliant safe joint, and then, Section III details system mathematical modeling and control method. In Section IV, we validate the control method through experiments with the compliant safe joint prototype and report an ex vivo experiment. Limitations and future improvements are discussed in Section V.

All the authors are with the Department of Mechanical and Automation Engineering, The Chinese University of Hong Kong, HKSAR; Corresponding author e-mail: zrwang[at]mae.cuhk.edu.hk.

This work is supported in part by the Hong Kong Research Grants Council under grants 415011 and CUHK6/CRF/13G and the Hong Kong Innovation and Technology Fund under ITS/020/12FP.

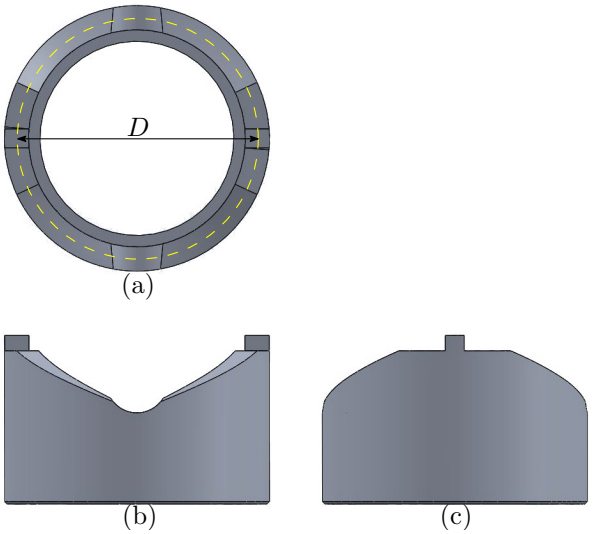

Fig. 2. Three view drawing of the CAD model of the stationary bridge: (a): top view, (b): front view and (c) left view. In the figure, $D = 47$mm (Diameter of the CSJ is 60mm).

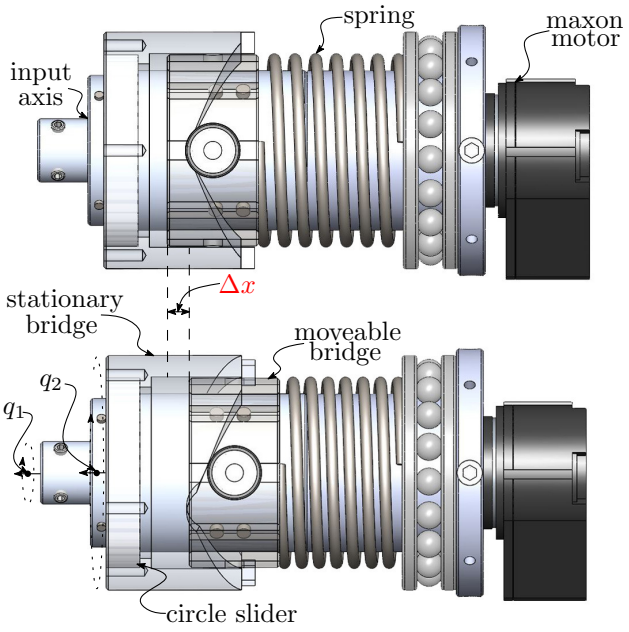

Fig. 3. CAD models of the CSJ working with work load smaller than the threshold (top) and with work load exceeding the threshold (bottom).

II. Design of Compliant Safe Joint

A. General Design Concept

The design of the compliant safe joint (CSJ) is presented in this section. The CSJ is designed for DC-motors with a high gear ratio and the main concept is to convert the axial motion into a circumferential motion by a transmission mechanism named bridge, which consists of two parts: movable bridge and stationary bridge. The movable bridge can only move along axial direction of motor and the stationary bridge can only rotate around the motor. We use bearings mounted on the movable bridge as wheels sliding along the helicoid surface of the stationary bridge which converts the axial compliance into circumferential compliance. Under normal situation, the bearings between the movable and stationary bridges are constrained in slots of the stationary bridge. When the torque exceeds a pre-defined threshold, the bearings will go out and then move along the helicoid surface. Simultaneously, the movable bridge will be pushed backward while the spring is compressed. Stiffness of the spring can be changed by adjusting the pre-load. Details are shown in Fig. 1.

B. Generating Compliance with the Bridge

Compliance of the CSJ is essentially generated by a linear spring. However, we need convert the linear compliance into the circumferential compliance, so that we can employ CSJ for surgical robot applications. The input axis, fixed on the motor output shaft, has eight holes distributed on its side surface. Installing keys into these holes builds four linear sliders for the movable bridge moving along the axial direction of the input axis. Two bearings, which are mounted on the movable bridge, contact with the stationary bridge on the slot and helicoid surface. The stationary bridge, mounted on the input axis by a circular slider, can only rotate with respect to the input axis, but cannot move along the axial direction of the input axis.

When the CSJ works like a rigid joint, which means its work load is smaller than the threshold, the bridges (both stationary and movable) are relatively static with respect to the motor shaft. When the work load increases and exceeds the threshold, the bearings, which are mounted on the movable bridge, go out of the stationary bridge's slots. Simultaneously, the stationary bridge has relative rotational motion and the movable bridge has relative axial linear motion with respect to the motor shaft respectively.

C. Rigid, Flexible and Free Region

There are totally six states from the bearing going out of the slot to the bearing reaching the mechanical limit. State 1 is rigid, states $1 \rightarrow 2$, $2 \rightarrow 3$, $3 \rightarrow 4$ are flexible, state $4 \rightarrow 5$ is free and state 5 is mechanical limit.

When the bearing is at state 1, the whole CSJ performs like a normal rigid joint. The CSJ has compliance when it is under states $1 \rightarrow 2$, $2 \rightarrow 3$, $3 \rightarrow 4$. The state $4 \rightarrow 5$ is free, which means that the motor's output torque cannot be transmitted through the bridge to the output shaft of the CSJ. The state 5 should be avoided, because the maximum output torque of CSJ is the same with that of the motor, and a impulse will be generated when the bearing reaches the mechanical limit, which is dangerous.

III. Controlling the Compliant Safe Joint

A. Notation

Column vectors and matrices are denoted by lower and upper case bold letters respectively, e.g., $\mathbf{v} \in \mathbb{R}^n$ and $\mathbf{M} \in \mathbb{R}^{p \times q}$. The diagonal matrices are represented by $diag(...)$.

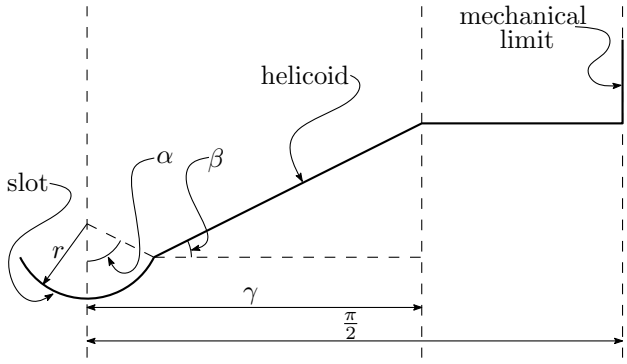

Fig. 4. Schematic diagram of the stationary bridge. Only one quarter of the hollow cylinder is sketched in an unfolding view. The black solid arc and lines represent slot and helicoid surface of stationary bridge, respectively. The black dashed lines are used as auxiliary lines.

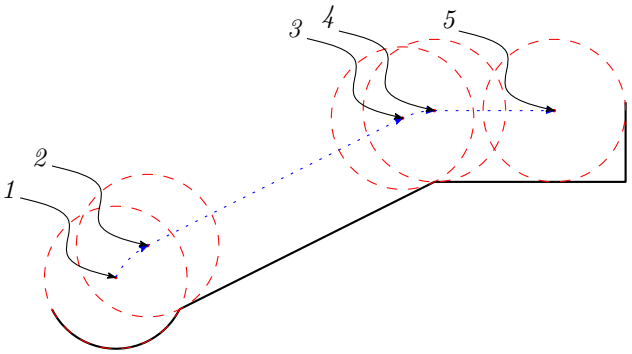

Fig. 5. Schematic diagram of all characteristic positions of the bearing moving along the surface of the stationary bridge. The black solid arc and lines represent the slot and helicoid surface of the stationary bridge, respectively. The red dashed circles and points represent the bearings and their center points, respectively. The blue dotted arc and lines represent the trajectory of the bearing's center.

B. Modeling

1) Flexible States: Let q_1 and q_2 be the angular position of the motor and the joint respectively. And define a column vector $\mathbf{q}$ having q_1 and q_2 as its components, i.e., $\mathbf{q} = \begin{bmatrix} q_1 & q_2 \end{bmatrix}^\intercal$. Let scalar $\delta = \begin{bmatrix} 1 & -1 \end{bmatrix} \mathbf{q}$ be the angular position difference between the motor and the joint. Let I_m and I_l be the moment of inertia of the motor and the link bar respectively. And define a matrix $\mathbf{I} = diag(I_m,\ I_l)$.

Let k be the stiffness coefficient. Let d and b be the joint and motor damping coefficient respectively. And let $\mathbf{K}$ be the stiffness coefficient matrix. Let $\mathbf{D}$ and $\mathbf{B}$ be the damping coefficient matrix of the joint and motor respectively, i.e.

$$\mathbf{K} = \begin{bmatrix} k & -k \\ -k & k \end{bmatrix}, \tag{1}$$

$$\mathbf{D} = \begin{bmatrix} d & -d \\ -d & d \end{bmatrix}, \tag{2}$$

$$\mathbf{B} = \begin{bmatrix} b & 0 \\ 0 & 0 \end{bmatrix}. \tag{3}$$

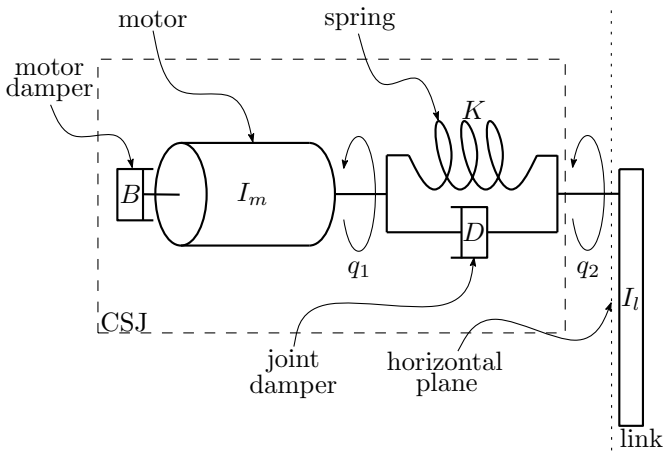

Fig. 6. Schematic diagram of a CSJ with one link bar.

Let u be the motor input of the joint and define $\boldsymbol{u}$ as follows

$$\boldsymbol{u} = \begin{bmatrix} u \\ 0 \end{bmatrix}. \tag{4}$$

With the parameters defined above, the equation of motion of the CSJ at the flexible states can be derived as follows using Euler-Lagrange Equation:

- $1 \to 2$, $2 \to 3$ and $3 \to 4$:

$$\mathbf{I}\ddot{\mathbf{q}} + \mathbf{D}_{i,i+1}\dot{\mathbf{q}} + \mathbf{B}\dot{\mathbf{q}} + \mathbf{K}_{i,i+1}\mathbf{q} = \boldsymbol{u}, \tag{5}$$

where $D_{i,i+1}$ and $K_{i,i+1}$, $i \in \{1,\ 2,\ 3\}$, are the joint damping coefficient matrix and stiffness coefficient matrix at the state $i \to i+1$ respectively.

However, in Fig 5, we notice that the two flexible states (i.e., $1 \to 2$ and $3 \to 4$) are narrow and the main flexible state is $2 \to 3$. Therefore, we can regard the two states as state-shift indicators rather than normal flexible states.

After approximation, the equation of motion of the joint at flexible state can be unified as follows:

$$\mathbf{I}\ddot{\mathbf{q}} + \mathbf{D}\dot{\mathbf{q}} + \mathbf{B}\dot{\mathbf{q}} + \mathbf{K}\mathbf{q} = \boldsymbol{u}. \tag{6}$$

2) Rigid State: the rigid state implicitly indicates that $q_1 = q_2 = q$. So the equation of motion can be given as follows:

- 1:

$$(I_m + I_l)\ddot{q} + b\dot{q} = u. \tag{7}$$

3) Free State: when joint is under the free state, the output torque cannot be transmitted to the link bar. The equation of motion is given as follows:

- $4 \to 5$:

$$I_m\ddot{q}_1 + b\dot{q}_1 = u. \tag{8}$$

C. Switching Algorithm

This subsection describes a switching algorithm for choosing appropriate controllers for different states.

Problem 1: Design a switching algorithm which can monitor state of the CSJ by using the state-shift indicators mentioned in the Subsection III-B, and choose corresponding controllers for the CSJ working under different states.

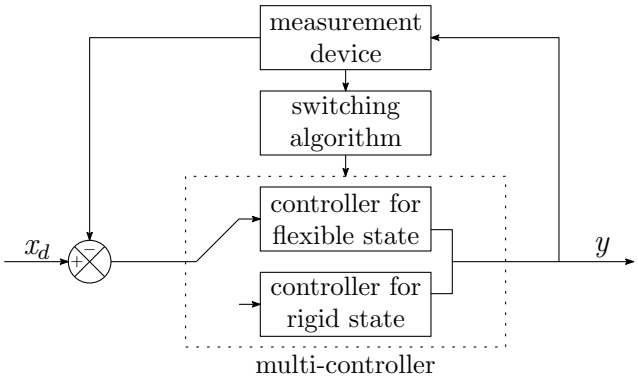

Fig. 7. Block diagram of the state feedback control with the multi-controller and switching algorithm.

According to Fig. 4 and 5, we can derive the state shift indicators by using geometric relationship. We can summarize the indicators as follows

$$\begin{aligned} \text{rigid:} \quad & \delta = 0 \\ \text{rigid} \leftrightarrow \text{flexible:} \quad & \delta \in \left(0, \tfrac{2r}{D}(sin\alpha - sin\beta)\right) \\ \text{flexible} \leftrightarrow \text{free:} \quad & \delta \in \left(\gamma - \tfrac{2r}{D} sin\beta), \gamma\right) \\ \text{mechanical limit:} \quad & \delta = \tfrac{\pi}{2} - \tfrac{2r}{D} \end{aligned}$$

With the state-shift indicators, we can develop a state feedback control method, shown in Fig. 7, in which we choose corresponding controller by judging which set the δ is in.

D. Trajectory Tracking Controller

This subsection describes a controller for the CSJ working under the rigid state.

Problem 2: Design an adaptive controller to asymptotically track a desired trajectory $q_d(t)$ without specific knowledge of the system parameters $\mathbf{a} \in \mathbb{R}^n$.

To cope with this issue, we use the model-based adaptive controller that estimates the unknown physical parameters on-line by an adaptive algorithm.

The control law is given by

$$u = \mathbf{y}(\dot{q}, \ddot{q}_r)\hat{\mathbf{a}} - K_D s, \tag{9}$$

with the adaptation law

$$\dot{\hat{\mathbf{a}}} = -P\mathbf{y}^\intercal s, \tag{10}$$

where $\mathbf{y} \in \mathbb{R}^n$ is regression vector, in the scalar situation, $\hat{\mathbf{a}} \in \mathbb{R}^n$ denotes estimated value of $\mathbf{a}$, K_D is a positive scalar, P is a symmetric positive definite matrix, and $s = \dot{\Delta}q + \lambda\Delta q = \dot{q} - \dot{q_r}$ ($\Delta q = q - q_d$) denotes the combined tracking error with $\lambda > 0$.

We now analyze the stability of the adaptive control method given above.

Proposition 1: For the dynamics (7), the control law (9) with adaption law (10) enforces asymptotic stability of the tracking error Δq.

Proof: Introduce a scalar function V as below

$$V = \frac{1}{2}\left(I_m + I_l\right)s^2 + \frac{1}{2}\tilde{\mathbf{a}}^\intercal P^{-1}\tilde{\mathbf{a}} \geq 0, \tag{11}$$

where $\tilde{\mathbf{a}} = \hat{\mathbf{a}} - \mathbf{a}$, and the derivative of V can be derived as follows

$$\begin{aligned} \dot{V} &= s\left\{u - [b\dot{q} + (I_m + I_l)\ddot{q}_r]\right\} + \dot{\hat{\mathbf{a}}}^\intercal P^{-1}\tilde{\mathbf{a}} && (12) \\ &= s\left(u - \mathbf{y}\mathbf{a}\right) + \dot{\hat{\mathbf{a}}}^\intercal P^{-1}\tilde{\mathbf{a}}, && (13) \end{aligned}$$

with the adaptive control law (9, 10)

$$\dot{V} = -K_D s^2 \leq 0. \tag{14}$$

Therefore, the scalar function V qualifies as a Lyapunov function for the system (7), i.e., CSJ works under rigid state. Because V is lower bounded, $\dot{V} \leq 0$ and $\ddot{V}$ is bounded, the asymptotic stability of the system can be given using Barbalat Lemma [18]. ■

E. Torque Regulation Controller

This subsection describes a controller for the CSJ working under the flexible state.

Problem 3: Design a dynamic state feedback controller, which can regulate the CSJ's output torque τ asymptotically by iteratively estimating the unknown system parameters $\mathbf{a} \in \mathbb{R}^n$.

The problem is indeed to finish a position tracking task, i.e., to converge to a constant or *slowly* varying target τ_d. We assume that the stiffness coefficient κ is exactly known such that the output torque τ can be computed from the angular position difference δ, i.e.,

$$\tau = \kappa\delta. \tag{15}$$

To cope with this issue, we introduce the adaptive control input as follows:

$$u = \mathbf{y}(\tau, \dot{q_1}, \dot{\tau}, \ddot{\tau}_r)\hat{\mathbf{a}} - K_D s, \tag{16}$$

with the adaptation law

$$\dot{\hat{\mathbf{a}}} = -P\mathbf{y}^\intercal s, \tag{17}$$

where $\mathbf{y} \in \mathbb{R}^n$ is regression vector, in the situation of 1 DOF, $\hat{\mathbf{a}} \in \mathbb{R}^n$ denotes estimated value of $\mathbf{a}$, K_D is a positive scalar, P is a symmetric positive definite matrix, and $s = \dot{\Delta\tau} + \lambda\Delta\tau = \dot{\tau} - \dot{\tau_r}$ ($\Delta\tau = \tau - \tau_d$) denotes the combined tracking error with $\lambda > 0$.

Proposition 2: For the approximation dynamics (6), the control law (16) with adaption law (17) leads to the tracking error $\Delta\tau$ asymptotically converge to zero.

Proof: Multiplying both sides of Equation (6) with $[1 \ -I_m/I_l]$ yields a scalar function:

$$\zeta_m\ddot{\tau} + \zeta_d\dot{\tau} + \zeta_k\tau = u - b\dot{q_1}, \tag{18}$$

where $\zeta_m = \frac{I_m}{\kappa}$, $\zeta_d = \frac{I_m + I_l}{I_l\kappa}d$ and $\zeta_k = \frac{I_m + I_l}{I_l\kappa}k$.

If we define a scalar function V as below

$$V = \frac{1}{2}\zeta_m s^2 + \frac{1}{2}\tilde{\mathbf{a}}^\intercal P^{-1}\tilde{\mathbf{a}} \geq 0, \tag{19}$$

where $\tilde{\mathbf{a}} = \hat{\mathbf{a}} - \mathbf{a}$, and the derivative of V can be derived as follows:

$$\begin{aligned} \dot{V} &= s\left[u - (\zeta_k\tau + b\dot{q_1} + \zeta_d\dot{\tau} + \zeta_m\ddot{\tau}_r)\right] + \dot{\hat{\mathbf{a}}}^\intercal P^{-1}\tilde{\mathbf{a}} && (20) \\ &= s\left(u - \mathbf{y}\mathbf{a}\right) + \dot{\hat{\mathbf{a}}}^\intercal P^{-1}\tilde{\mathbf{a}}, && (21) \end{aligned}$$

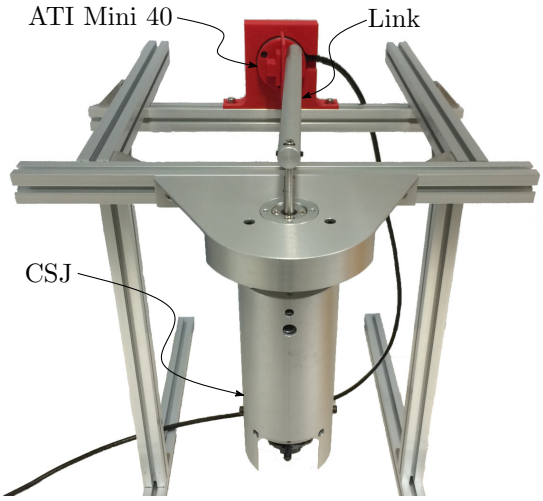

Fig. 8. The experimental setup. An ATI force sensor is used to measure the contact force.

with the adaptive control law (16, 17)

$$\dot{V} = -K_D s^2 \leq 0. \tag{22}$$

Therefore, the scalar function V qualifies as a Lyapunov function for the system (6), i.e., the CSJ works under the flexible state, and the asymptotic stability of the system can be given using Krasovskii-LaSalle Theorem [18]. ■

IV. Experiments

In this section, we present a experimental study to evaluate both design and control methods of the CSJ. In the experiment, we used a one degree-of-freedom robot manipulator with the CSJ acting as actuator to accomplish several tasks, in which the CSJ needs to track a specific trajectory in the rigid state and also push a rigid surface with the desired contact force in the flexible state. Finally, we report an ex vivo experiment, in which our surgical robot, the uterus manipulator, was actuated by the CSJs.

A. Experiment Setup

In order to command the torque u of the motor, we use a Galil DMC-1842, configured in the current mode, along with a Maxon 4-Q-Servoamplifier. With two encoders with 500 PPR resolution being mounted on the motor bottom and the CSJ output axis respectively, and the control system providing 12 MHz sample rate, we can obtain accurate position and velocity information. Fig. 8 shows details of the experimental setup.

B. Parameter Identification

Because we made the assumption that the stiffness coefficient κ in the Equation (15) is exactly known, we must experimentally identify the value of κ by using the standard linear regression method. The result is $\kappa = 0.02712$ Nm/deg.

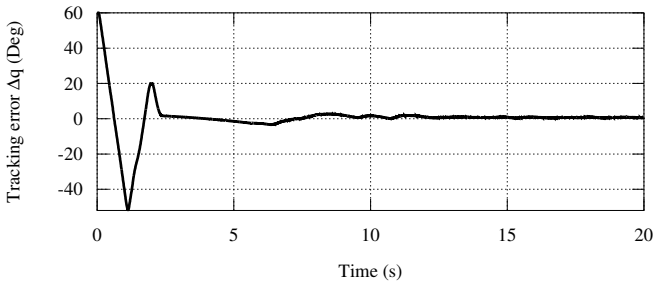

Fig. 9. Trajectory tracking error $\Delta q = q - q_d$. Note that we used q_2, i.e., output of CSJ, in the experiment.

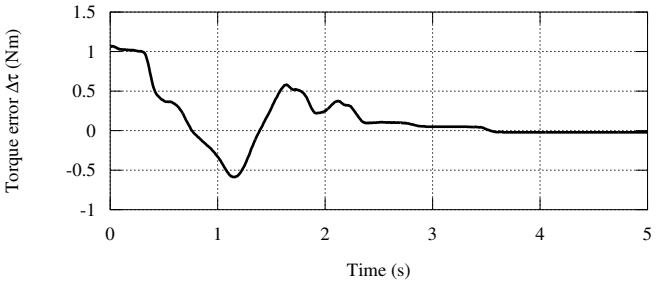

Fig. 10. Magnitude of measured torque error $\Delta\tau$.

C. Experiment Results

When the CSJ works under the rigid state, we set the desired trajectory as $q_d = Asin(\omega t + \phi)$, where $A = 60$ deg, $\omega = \frac{\pi}{5}$ and $\phi = \frac{3\pi}{2}$ deg. The trajectory tracking error is shown in Fig. 9. The profiles shown in the figure experimentally corroborate that the control method can track the trajectory asymptotically.

When the CSJ works under the flexible state, we set the desired torque as $\tau_d = 1$ Nm. Fig. 10 shows the asymptotic minimization of the measure torque error. The results experimentally prove our torque regulation method can asymptotically regulate the output torque of CSJ.

Note that, in the trajectory tracking experiment, our controller is designed for trajectory tracking task, i.e., following a time-varying reference. However, in the torque regulation experiment, our controller is designed for set-point regulation task, i.e., converging to a constant or slowly varying references.

D. Ex Vivo Experiment

We used our CSJs in an ex vivo experiment with a uterus manipulation surgical robot for hysterectomy surgery. The robot has 4 degrees of freedom with its first two joints actuated by CSJs as shown in Fig. 11.

The first and second joints move along yaw and pitch direction of the uterus manipulator, respectively. During the experiment, surgeons tested the robot by trying to hold the cadaver's uterus in different positions with the manipulator.

A force transducer was installed in the middle part of the manipulator, so that the interaction force could be obtained in real time. When the manipulator reached dangerous region, i.e., the interaction force exceeds the safety threshold value,

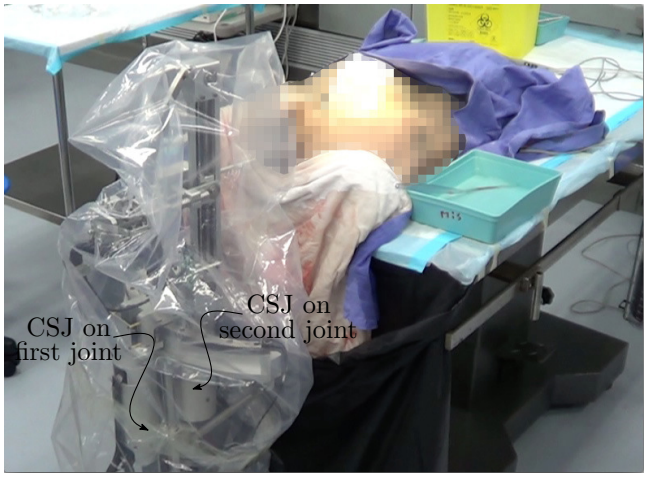

Fig. 11. Ex vivo experiment.

we tuned the thresholds of the CSJs to guarantee that the CSJs would shift into the flexible states.

During the whole ex vivo experiment, the CSJs worked well under the rigid state and could shift into the flexible state when the interaction force exceeded the safety threshold recommended by surgeons.

V. Conclusion

In this paper, we first introduced a design of novel compliant safe joint. The CSJ can work as a normal rigid joint when the work load under a pre-defined threshold and have compliance when the load exceeds the threshold. Then, because the mechanical structure will change when the CSJ works under different states, we introduced different control methods for rigid and flexible states respectively, and used a switching algorithm to select appropriate controllers under different states. Next, we validated the proposed design concept and control methods by experiments with a one-degree-freedom manipulator actuated by the CSJ. Finally, we reported an ex vivo experiment, in which we tested the performance of the CSJs.

In contrast with other flexible or compliant joints, the CSJ introduced in this paper is more compact such that it can be easily implemented in the real application. Moreover, the compliance will only appear when needed, i.e., when the work load exceeds a pre-defined threshold.

In the future, we plan to develop multi-degree-freedom robot manipulator with the CSJs and design the control algorithm with the nonlinear dynamics of the robot manipulate is taken into account.

References

[1] Y. Yamada, Y. Hirasawa, S. Huang, Y. Umetani, and K. Suita, "Human-robot contact in the safeguarding space," *Mechatronics, IEEE/ASME Transactions on*, vol. 2, no. 4, pp. 230–236, 1997.

[2] A. Bicchi, M. A. Peshkin, and J. E. Colgate, "Safety for physical human–robot interaction," *Springer handbook of robotics*, pp. 1335–1348, 2008.

[3] A. Bicchi, M. Bavaro, G. Boccadamo, D. De Carli, R. Filippini, G. Grioli, M. Piccigallo, A. Rosi, R. Schiavi, S. Sen, *et al.*, "Physical human-robot interaction: Dependability, safety, and performance," in *Advanced Motion Control, 2008. AMC'08. 10th IEEE International Workshop on*. IEEE, 2008, pp. 9–14.

[4] C. A. Klein and R. L. Briggs, "Use of active compliance in the control of legged vehicles," *Systems, Man and Cybernetics, IEEE Transactions on*, vol. 10, no. 7, pp. 393–400, 1980.

[5] B. R. Shetty and V. Ang, "Active compliance control of a puma 560 robot," in *Robotics and Automation, 1996. Proceedings., 1996 IEEE International Conference on*, vol. 4. IEEE, 1996, pp. 3720–3725.

[6] W. Wang, R. N. Loh, and E. Y. Gu, "Passive compliance versus active compliance in robot-based automated assembly systems," *Industrial Robot: An International Journal*, vol. 25, no. 1, pp. 48–57, 1998.

[7] M. W. Spong, "Modeling and control of elastic joint robots," *Journal of dynamic systems, measurement, and control*, vol. 109, no. 4, pp. 310–318, 1987.

[8] P. Tomei, "A simple pd controller for robots with elastic joints," *Automatic Control, IEEE Transactions on*, vol. 36, no. 10, pp. 1208–1213, 1991.

[9] A. De Luca and P. Lucibello, "A general algorithm for dynamic feedback linearization of robots with elastic joints," in *Robotics and Automation, 1998. Proceedings. 1998 IEEE International Conference on*, vol. 1. IEEE, 1998, pp. 504–510.

[10] H. Vallery, R. Ekkelenkamp, H. Van Der Kooij, and M. Buss, "Passive and accurate torque control of series elastic actuators," in *Intelligent Robots and Systems, 2007. IROS 2007. IEEE/RSJ International Conference on*. IEEE, 2007, pp. 3534–3538.

[11] G. A. Pratt and M. M. Williamson, "Series elastic actuators," in *Intelligent Robots and Systems 95.'Human Robot Interaction and Cooperative Robots', Proceedings. 1995 IEEE/RSJ International Conference on*, vol. 1. IEEE, 1995, pp. 399–406.

[12] C. English and D. Russell, "Implementation of variable joint stiffness through antagonistic actuation using rolamite springs," *Mechanism and Machine Theory*, vol. 34, no. 1, pp. 27–40, 1999.

[13] R. Van Ham, B. Vanderborght, M. Van Damme, B. Verrelst, and D. Lefeber, "Maccepa, the mechanically adjustable compliance and controllable equilibrium position actuator: Design and implementation in a biped robot," *Robotics and Autonomous Systems*, vol. 55, no. 10, pp. 761–768, 2007.

[14] R. v. Ham, T. G. Sugar, B. Vanderborght, K. W. Hollander, and D. Lefeber, "Compliant actuator designs," *Robotics & Automation Magazine, IEEE*, vol. 16, no. 3, pp. 81–94, 2009.

[15] J. Choi, S. Hong, W. Lee, S. Kang, and M. Kim, "A robot joint with variable stiffness using leaf springs," *Robotics, IEEE Transactions on*, vol. 27, no. 2, pp. 229–238, 2011.

[16] F. Flacco, A. De Luca, I. Sardellitti, and N. G. Tsagarakis, "On-line estimation of variable stiffness in flexible robot joints," *The International Journal of Robotics Research*, vol. 31, no. 13, pp. 1556–1577, Nov. 2012.

[17] K. Koganezawa, H. Inomata, and T. Nakazawa, "Actuator with non-linear elastic system and its application to 3 dof wrist joint," in *Mechatronics and Automation, 2005 IEEE International Conference*, vol. 3. IEEE, 2005, pp. 1253–1260.

[18] J.-J. E. Slotine and W. Li, *Applied nonlinear control*. Prentice-Hall Englewood Cliffs, NJ, 1991, vol. 199, no. 1.